

An Investigation of Quantum States in Ultra-Small InAs/GaAs Quantum Dots by Means of Photoluminescence

C. H. Wu,¹ Y. G. Lin,¹ S. L. Tyan,^{1,*} S. D. Lin,² and C. P. Lee³

¹*Department of Physics, National Cheng Kung University, Tainan, Taiwan, ROC*

²*Cavendish Laboratory, University of Cambridge,
Madingley Road, Cambridge CB3 0HE, UK*

³*Department of Electronics Engineering,
National Chiao Tung University, Hsinchu, Taiwan, ROC*

(Received January 17, 2005)

The quantum states of InAs/GaAs quantum dots (QDs) with a base length of less than 10 nm are studied by means of excitation and temperature dependent photoluminescence (PL). The base length of the QDs, calculated by the PL ground state transition energy, is in agreement with the atomic force microscopy measurements. By means of the excitation-dependent PL, we demonstrate that only the ground electron and hole states exist when the base length of the QDs is smaller than about 7.3 nm, whereas larger dots, with a base length of about 8.7 nm, give rise to one excited hole state. The measured energy separation between the ground and the excited hole states is in good agreement with the theoretical calculation. The transition energy in the temperature-dependent PL spectra shows a rapid redshift as the temperature is raised higher than the critical temperature. The redshift rate is about 2.8 and 2.5 times larger than the values calculated by Varshni's law for small and large dots, respectively. The higher redshift rate can be explained by the stronger tunneling effect. In addition, the PL linewidths show a V-shaped dependence on the temperature. This behavior can be described as a tunneling and electron-phonon scattering effect.

PACS numbers: 78.55.-m, 78.55.Cr, 78.67.Hc

I. INTRODUCTION

The quantum dot (QD) based structures are of much interest today for both physics and potential applications, due to the δ -function-like density of the state and the strong confinement of the electron and hole wave functions. For example, the much lower threshold current and higher optical gain, compared to that of a quantum well (QW), enable QDs to improve the performance of optoelectronic devices, such as lasers [1] and detectors [2]. The lower scattering probability during the transport process allows them to be used as single electron transistors [3]. The ideal QD for a quantum logic gate in a quantum computer has evoked extensive discussion [4].

Uniformity is a great challenge in the growth of QDs. Recently, a narrow photoluminescence (PL) linewidth of 16.5 meV was achieved for QDs grown by the Stranski-Krastanov (SK) mode [5]. In order to meet the requirements of optical communication, much effort has been devoted to growing larger size quantum dots [6, 7]. Studies of theoretical calculations [8, 9] and experimental measurements [6, 10] concerned with QDs having a base length

larger than 10 nm have been made. However, to the best of our knowledge, there is little experimental information dealing with ultra small QDs. Nevertheless, these smaller dots are helpful for understanding the characteristics of the three-dimensional (3D) confinement structures, because the unexpected interactions between carriers in the same dot can be excluded.

In this article, we study the excitation- and temperature-dependent PL spectra of ultra small InAs/GaAs QDs with base lengths of less than 10 nm. The dot's base length was calculated by the energy of the ground state transition, and it was confirmed by the atomic force microscopy (AFM) technique. The excitation-dependent PL spectra demonstrated that only ground electron and hole states exist in InAs QDs with a base length of ~ 7.3 nm. As the base length increases to ~ 8.7 nm, one excited hole state is exhibited. In addition, from the temperature-dependent PL spectra, we find that the tunneling effect and the electron-phonon scattering are stronger in smaller dots.

II. SAMPLES AND EXPERIMENTS

The two samples used in this study were grown by molecular beam epitaxy on (001) GaAs substrate in a Varian GEN II reactor. For sample A, a 10 nm GaAs buffer layer was grown on the substrate followed by 5-period 2 nm $\text{Al}_{0.3}\text{Ga}_{0.7}\text{As}$ /2 nm GaAs superlattice (SL). The QD layer was then added by depositing a 2.4 InAs monolayer (ML) with a growth rate of 0.05 ML/s, an As_4 partial pressure of 2.7×10^{-5} Torr, and a substrate temperature of 480°C . This was followed by the deposition of a 100 nm GaAs layer. Then a 5-period 2 nm GaAs/2 nm $\text{Al}_{0.3}\text{Ga}_{0.7}\text{As}$ SL and a 20 nm GaAs capping layer was grown. For sample B, first a 20 nm $\text{Al}_{0.5}\text{Ga}_{0.5}\text{As}$ layer was grown on the substrate, then a 150 nm GaAs layer was added. Subsequently the QD layer was formed by the deposition of a 2.6 InAs monolayer using the same growth rate and temperature as sample A, but with a different arsenic mode, As_2 , and with a lower partial pressure of 1.6×10^{-5} Torr. After this a 200 nm $\text{Al}_{0.5}\text{Ga}_{0.5}\text{As}$ layer was deposited, followed by the 20 nm GaAs capping layer. The growth temperature for all the structures was 580°C , except for when the QD layer was being grown. For the purpose of AFM measurements, another InAs QD layer was grown, using the same growth conditions, on top of each sample.

For the PL measurement the sample was excited by an He-Ne laser (633 nm). The collected PL was dispersed through a 0.55 m monochromator, and then detected with an InGaAs detector. The temperature-dependence of the PL measurements were performed in a close-cycle He cryostat with an illuminating power of 2.4 mW and a spot radius of 0.35 mm. The excitation-dependent PL spectra were measured at 20 K. A laser beam with a power of 3.8 mW was focused on a spot with a radius of 10 μm . The excitation intensity was varied from 0.6 W/cm^2 to 1.2 kW/cm^2 by a neutral density filter.

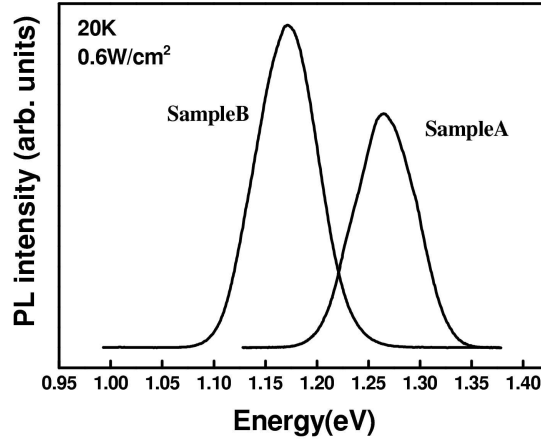


FIG. 1: The PL spectra for sample A and sample B at 20 K under an excitation intensity of 0.6 W/cm².

III. RESULTS AND DISCUSSIONS

III-1. AFM and theoretical calculations

The PL spectra measured under a low excitation power of 0.6 W/cm² at 20 K are shown in Fig. 1. The ground state transition energy of sample A, obtained by the Gaussian lineshape fit, is 1.265 eV, which is higher than that of sample B, 1.172 eV, while the full width at half maximum (FWHM) for the two samples are almost the same, ~ 59 meV. This same FWHM value indicates a similar QD size distribution for the two samples. The relationship between the QD transition energy and base length can be solved based on the three-dimensional single particle effective mass Schrödinger equation using a locally varying, anisotropic effective mass, as reported by M. Grundmann *et al.* [11–13]. According to this theory, the dot base lengths are ~ 7.3 nm and ~ 8.7 nm for samples A and B, respectively. We also performed the AFM measurements on equivalent uncapped dots. Only the image of sample A is shown in Fig. 2. It reveals a uniform QD size distribution. The average base lengths of the islands measured from each image are 8 nm and 9.5 nm, with a dot density of 1.3×10^{11} cm⁻² and 3.6×10^{11} cm⁻² for samples A and B, respectively.

The size of the InAs islands, deduced from the transition energy, is smaller than that of the uncapped QD layer measured by the AFM technique, this is due to the quenching of their evolution by the GaAs deposits [14]. The lower dot density and the relatively small base length of sample A are probably due to the larger driving force, from the greater amount of As deposition for the corrugation of the InAs wetting layer (WL) [15], which retarded the development of the dots.

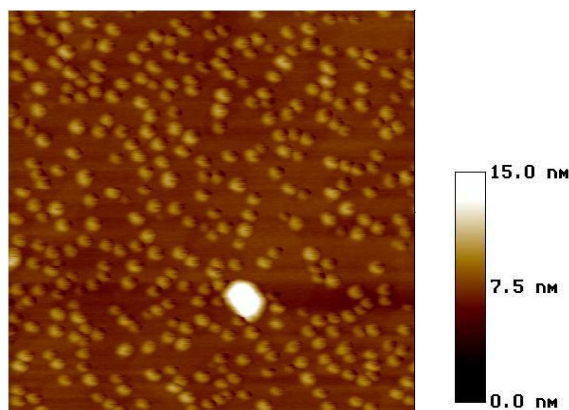


FIG. 2: The AFM image ($0.5 \mu\text{m} \times 0.5 \mu\text{m}$) of sample A.

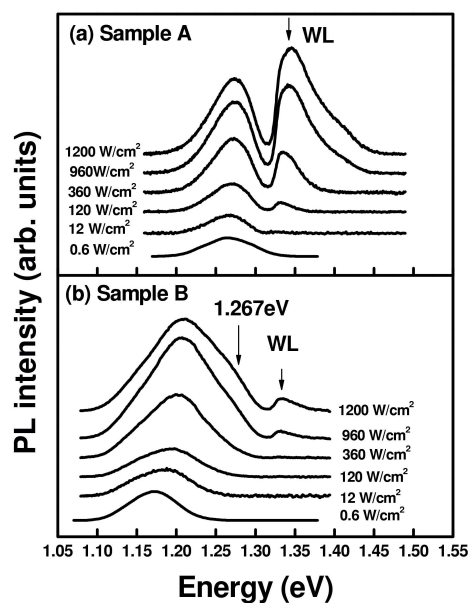


FIG. 3: The excitation-dependent PL spectra of (a) sample A and (b) sample B.

III-2. Excitation-dependent PL

Fig. 3 shows the PL spectra for both samples under an excitation intensity varying from 0.6 W/cm^2 to 1.2 kW/cm^2 at 20 K . In Fig. 3(a), there is only the ground state transition at the energy position of 1.265 eV under the lowest excitation intensity of 0.6 W/cm^2 . A new feature arises at about 1.34 eV , when the excitation intensity becomes larger than 12 W/cm^2 . A similar phenomena can be seen in Fig. 3(b). The ground state transition exists at 1.172 eV under the lowest excitation intensity, and a new structure arises when the

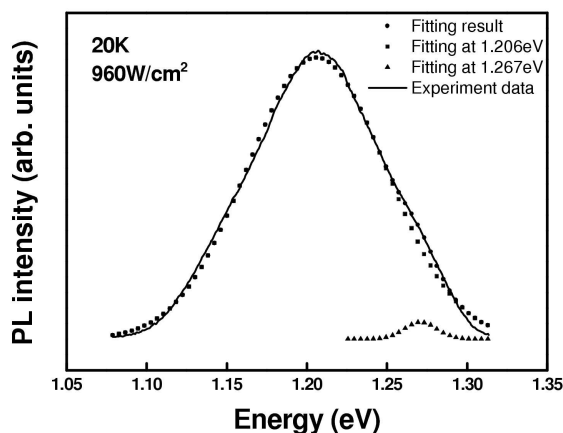


FIG. 4: The Gaussian lineshape fit for the PL spectrum of sample B under saturated excitation intensity.

excitation intensity reaches 960 W/cm^2 . It is evident that for both samples the low-energy side of the peak around 1.34 eV remains almost unchanged, while the high-energy side becomes much longer as the excitation intensity increases. This is a typical characteristic of the QW continuum state [16, 17] and corresponds to the InAs WL transition. The WL transition occurs only after all states in the dots are saturated. The excitation intensities of 12 W/cm^2 and 960 W/cm^2 therefore correspond to the saturation excitation intensity for samples A and B, respectively.

In Fig. 3(a), the occurrence of the WL transition is because all the ground states of the QDs are filled as the excitation intensity reaches the saturated excitation intensity; surplus carriers can only occupy the WL state. In addition, no other peak arises in the PL spectrum, even when the sample was excited under an intensity of up to 1.2 kW/cm^2 . This proves that no excited electron or hole state transition is involved in such small QDs, which is in good agreement with the theoretical prediction, that there is no excited electron or hole state when the dot base length is smaller than 7.5 nm .

In contrast to sample A, sample B shows very different results. In Fig. 3(b), we can observe an ambiguous second peak positioned at an energy between the ground state transition energy and the typical WL transition, when the excitation intensity is increased to 960 W/cm^2 . The spectra with the WL transition excluded can be well deconvoluted by two Gaussian lineshapes, when the excitation intensity is higher than the saturated excitation intensity. The result for the spectrum obtained at the saturation intensity is shown in Fig. 4, and it fits very well. The ground state transition energy is shown to be 1.206 eV and the other transition energy is 1.267 eV . We calculated the energy separation between the ground and the excited hole state. The calculations show that there is only one excited hole state when the base length lies between 7.5 and 10.5 nm , according to Grundmann's theory [11–13]. This calculated value, 95 meV , is in good agreement with the energy difference between 1.267 eV and the ground state transition energy of 1.172 eV ,

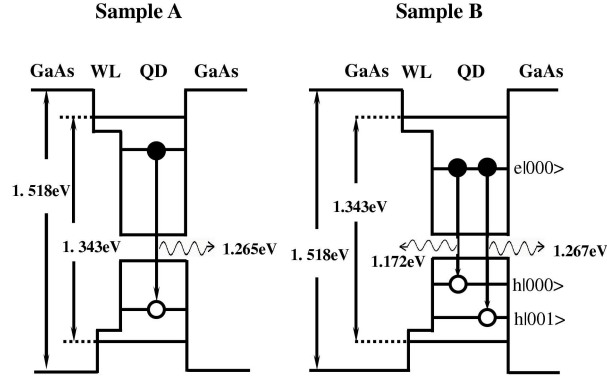


FIG. 5: The band diagrams for the two samples.

under the lowest excitation energy. Therefore, the peak at 1.267 eV could be designated as the transition from the ground electron state to the excited hole $|001\rangle$ state.

The band diagrams of the two samples, obtained from the measurements of the excitation-dependent PL, are plotted in Fig. 5. They show that only the ground state transition, ~ 1.265 eV, exists in sample A. The ground state transition, ~ 1.172 eV, with one excited state transition, ~ 1.267 eV, occurs in sample B. The electron ground state in sample A is higher and closer to the WL continuum state than that in sample B. The separation between the hole states in sample B is 95 meV.

Finally, it is noticeable that there is a significant blue shift (~ 37 meV) in the ground state transition in Fig. 3(b) when the excitation intensity increases from 0.6 W/cm² to 1.2 kW/cm². The asymmetrical broadening of the PL peak towards the higher energy can be attributed to the ground states of the larger dots being saturated, so the carriers recombined from the ground states of the smaller dots [18].

III-3. Temperature-dependent PL

The temperature-dependent PL spectra were observed at temperatures varying from 20 K to 210 K. The relative temperature-dependent peak positions for both samples are shown in Fig. 6(a). The relative peak positions show a sigmoid dependence on temperature for both samples. The two dotted lines separated by a constant energy indicate the relative energy position calculated by Varshni's law [19]. The coincidence of the experimental data and the calculated value at lower and higher temperatures is mainly due to the thermal expansion of the lattice constant [20]. When the temperature is lower than the critical temperature, 50 K and 80 K for samples A and B, respectively, the peak position is almost a constant, because the excitons are localized at a certain potential minimum and the carrier population is characterized by a non-equilibrium distribution [21, 22]. As the temperature becomes higher than the critical temperature, the relative peak positions show a rapid redshift. This behavior is due to the fact that the excitons are dissociated, because the thermal energy overcomes the exciton binding energy and then escapes to the nearby dots

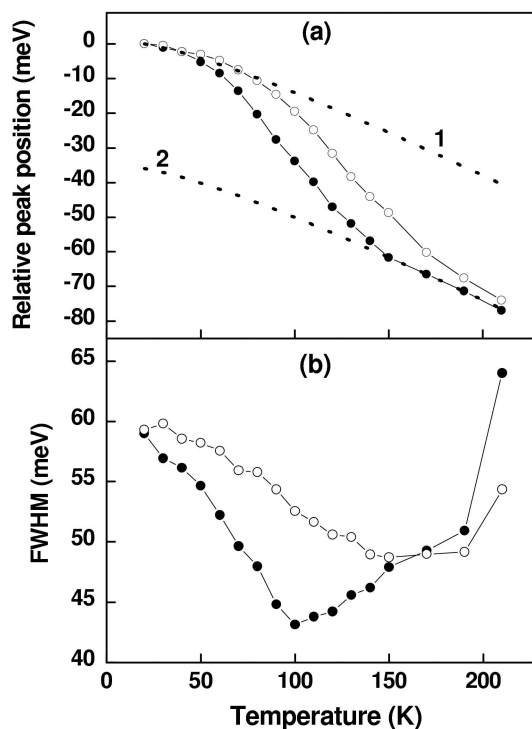


FIG. 6: The temperature dependence of (a) the relative peak position and (b) the FWHM for sample A (solid circles) and sample B (hollow circles). The dotted lines denoted as 1 and 2 in (a) are the values calculated by Varshni's law.

to recombine radiatively [21]. The carriers tend to redistribute in equilibrium and reveal a rapid redshift. The energy level of sample A is higher (as shown in Fig. 3), therefore the energy needed to escape from the dot is smaller. This will increase the tunneling probability and enhance the re-trapping process of the larger dots [23, 24]. This strong tunneling effect results in a faster energy shift of sample A. The rapid redshift rate is 0.77 and 0.69 meV/K for sample A (50 – 150 K) and sample B (80 – 170 K), respectively, which is larger than the typical redshift value, 0.28–0.41 meV/K, for QDs with a base length larger than 10 nm and about 2.8 and 2.5 times larger than the values calculated by Varshni's law.

The FWHMs at different temperatures for both samples are plotted in Fig. 6(b). We can see that the FWHM shows a dip at 100 K and 150 K for samples A and B, respectively. As discussed above, the carriers will tunnel to nearby dots and recombine radiatively at higher temperatures. This strong tunneling effect in sample A results in a larger FWHM reduction rate [23, 24]. In addition, for sample A (B) the FWHM is broadened when the temperature is higher than 100 K (150 K) because electron-phonon scattering dominates at the higher temperatures [10, 22–24]. The larger broadening rate indicates that the electron-phonon scattering is stronger. As is evident in this figure, the larger reduction and broadening rate reveals a stronger tunneling effect and electron-phonon scattering in

sample A, hence, smaller dots.

IV. CONCLUSIONS

In this paper we studied ultra small InAs QDs on a (001) GaAs substrate with a base length of about 7.3 nm and 8.7 nm, grown under the As₄ and As₂ mode respectively. The base length of the dots, as estimated by the PL ground state energy, is in agreement with the results obtained from the AFM measurement. From the excitation-dependent PL spectra, we demonstrate that there is no excited electron or hole state in dots with a base length of ~ 7.3 nm and only one excited hole $|001\rangle$ state exists in dots with a base length of ~ 8.7 nm. From the temperature-dependent PL spectra we can conclude that the tunneling effect and electron-phonon scattering play very important roles in such smaller dots. The stronger tunneling effect will result in a rapid redshift, about three times larger than the value calculated by Varshni's law. The strong tunneling effect will also result in a larger FWHM reduction rate. The electron-phonon scattering effect is stronger than the tunneling effect when the temperature is higher than 100 K, for dots with a base length of about 7.3 nm. The smaller the QD the stronger the tunneling effect and electron-phonon scattering.

Acknowledgments

This work was supported by the National Science Council of Taiwan, R.O.C, under Contract No. NSC 93-2119-M-006-011.

References

- * Corresponding author; Electronic address: sltyan@mail.ncku.edu.tw
- [1] G. T. Lin, A. Stintz, H. Li, K. J. Malloy, and L. F. Lester, *Electron. Lett.* **35**, 1163 (1999).
 - [2] S. Raghavan, D. Forman, P. Hill, N. R. Weisse-Bernstein, G. von Winckel, P. Rotella, S. Krishna, S. W. Kennerly, and J. W. Little, *J. Appl. Phys.* **96**, 1036 (2004).
 - [3] T. H. Wang, H. W. Li, and J. M. Zhou, *Appl. Phys. Lett.* **82**, 3092 (2003).
 - [4] A. Zrenner, E. Beham, S. Stuffer, F. Findeis, M. Bichler, and G. Abstreiter, *Nature* **418**, 612 (2002).
 - [5] Tao. Yang, Jun. Tatebayashi, Shiro. Tsukamoto, Masao. Nishioka, and Yasuhiko. Arakawa, *Appl. Phys. Lett.* **84**, 2817 (2004).
 - [6] Zhonghui Chen, O. Baklenov, E. T. Kim, I. Mukhametzhanov, J. Tie, A. Madhukar, Z. Ye, and J. C. Campbell, *J. Appl. Phys.* **89**, 4558 (2001).
 - [7] Eui-Tai Kim, Zhonghui Chen, and Anupam Madhukar, *Appl. Phys. Lett.* **81**, 3473 (2002).
 - [8] O. Stier, M. Grundmann, and D. Bimberg, *Phys. Rev. B* **59**, 5688 (1999).
 - [9] R. Heitz, I. Mukhametzhanov, O. Stier, A. Madhukar, and D. Bimberg, *Phys. Rev. Lett.* **83**, 4654 (1999).
 - [10] H. S. Lee, J. Y. Lee, and T. W. Kim, *J. Cry. Growth.* **258**, 256 (2003).

- [11] M. Grundmann, N. N. Ledentsov, O. Stier, D. Bimberg, V. M. Ustinov, P. S. Kop'ev, and Zh. I. Alferov, *Phys. Appl. Phys. Lett.* **68**, 979 (1996).
- [12] M. Grundmann, N. N. Ledentsov, O. Stier, J. Böhrer, and D. Bimberg, *Phys. Rev. B* **53**, 10509 (1996).
- [13] M. Grundmann, O. Stier, and D. Bimberg, *Phys. Rev. B* **52**, 11969 (1992).
- [14] J. Y. Marzin, J. M. Geraréd, A. Izraël, D. Barrier, and G. Bastard, *Phys. Rev. Lett.* **73**, 716 (1994).
- [15] J. D. Song, Y. M. Park, J. C. Shin, J. G. Lim, Y. J. Park, W. J. Choi, I. K. Han, and J. I. Lee, *J. Appl. Phys.* **96**, 4122 (2004).
- [16] K. Matsuda, K. Ikeda, T. Saiki, H. Saito, and K. Nishi, *Appl. Phys. Lett.* **83**, 2250 (2003).
- [17] P. G. Eliseev and I. V. Akimova, *Semiconductors* **32**, 423 (1998).
- [18] Yu. I. Mazur, W. Q. Ma, X. Wang, Z. M. Wang, G. J. Salamo, M. Xiao, T. D. Mishima, and M. B. Johnson, *Appl. Phys. Lett.* **83**, 987 (2003).
- [19] Z. M. Fang, K. Y. Ma, D. H. Jaw, R. M. Cohen, and G. N. Stringfellow, *J. Appl. Phys.* **67**, 7034 (1990).
- [20] M. L. Cohen and D. J. Chandi, in *Handbook on semiconductors* edited by M. Balkanski (North-Holland, New York, 1980), Vol. 2. Chap. 4B.
- [21] D. I. Lubyshev, P. P. Gonzalez-Borrero, E. Marega, Jr., E. Petitprez, N. La Scala, Jr., and P. Basmaji, *Appl. Phys. Lett.* **68**, 205 (1996).
- [22] W. H. Jiang, X. L. Ye, H. Z. Xu, D. Ding, J. B. Liang, and Z. G. Wang, *J. Appl. Phys.* **88**, 2529 (2000).
- [23] H. Kissel, U. Muller, C. Walther, W. T. Masselink, Yu. I. Mazur, G. G. Tarasov, and M. P. Lisitsa, *Phys. Rev. B* **62**, 7213 (2000).
- [24] Z. Y. Xu, Z. D. Lu, X. P. Yang, Z. L. Yuan, B.Z. Zheng, J. Z. Xu, W. K. Ge, Y. Wang, J. Wang, and L. L. Chang, *Phys. Rev. B* **54**, 11528 (1996).